



Published in final edited form as:

*J Immunol.* 2012 September 15; 189(6): 2985–2994. doi:10.4049/jimmunol.1200846.

## Opposing Roles for Complement Component C5a in Tumor Progression and the Tumor Microenvironment

Lacey Gunn<sup>\*,†,‡</sup>, Chuanlin Ding<sup>\*,‡</sup>, Min Liu<sup>\*</sup>, Yunfeng Ma<sup>\*</sup>, Chunjian Qi<sup>\*,§</sup>, Yihua Cai<sup>\*</sup>, Xiaoling Hu<sup>\*</sup>, Deep Aggarwal<sup>\*</sup>, Huang-ge Zhang<sup>\*,†</sup>, and Jun Yan<sup>\*,†</sup>

<sup>\*</sup>Division of Hematology/Oncology, Department of Medicine, James Graham Brown Cancer Center, University of Louisville, Louisville, KY, U.S.A

<sup>†</sup>Department of Microbiology and Immunology, University of Louisville School of Medicine, Louisville, KY, U.S.A

<sup>§</sup>Department of Oncology, The Affiliated Hospital of Nanjing Medical University, Changzhou No.2 People's Hospital, Changzhou, China

### Abstract

Promoting Complement (C) activation may enhance immunological mechanisms of anti-tumor antibodies for tumor destruction. However, C activation components, such as C5a, trigger inflammation which can promote tumor growth. We addressed the role of C5a on tumor growth by transfecting both human carcinoma and murine lymphoma with mouse C5a. *In vitro* growth kinetics of C5a, control vector (CV), or parental cells revealed no significant differences. Tumor-bearing mice with C5a-transfected xenografted tumor cells had significantly less tumor burden as compared to CV tumors. NK cells and macrophages infiltrated C5a expressing tumors with significantly greater frequency while VEGF, arginase, and TNF- $\alpha$  production were significantly less. Tumor-bearing mice with high C5a-producing syngeneic lymphoma cells had significantly accelerated tumor progression with more Gr-1<sup>+</sup>CD11b<sup>+</sup> myeloid cells in spleen and overall decreased CD4<sup>+</sup> and CD8<sup>+</sup> T cells in tumor, tumor-draining lymph nodes (TDLN), and spleen. In contrast, tumor-bearing mice with low C5a-producing lymphoma cells had a significantly reduced tumor burden with increased IFN- $\gamma$ -producing CD4<sup>+</sup> and CD8<sup>+</sup> T cells in spleen and TDLN. These studies suggest concentration of local C5a within the tumor microenvironment is critical in determining its role in tumor progression.

### Introduction

Complement (C) is an important component of the immune system, and activation of the C cascade occurs via three pathways (1). The C cascade is highly regulated at several levels by C regulatory proteins (CRPs), such as CD55 (2, 3). CD55 (decay-accelerating factor, DAF) is expressed on nearly all cells of the body and overexpressed on tumor cells, and is responsible for the accelerated dissolution of the C3 and C5 convertases and eliminates release of anaphylatoxins (2). C activation component C5a is a potent immune mediator, activating immune cells upon interaction with the C5a receptor (C5aR) resulting in oxidative burst in neutrophils, phagocytosis augmentation, and enzymatic granule release, as well as vasodilation of local blood vessels to enhance immune cell entry and exchange of cells and

Correspondence should be addressed to Jun Yan, M.D., Ph.D., Tumor Immunobiology Program, James Graham Brown Cancer Center, Clinical & Translational Research Building, Rm 319, University of Louisville, 505 South Hancock Street, Louisville, KY 40202, Tel: 502 852-3628, Fax: 502 852-2123, jun.yan@louisville.edu.

<sup>‡</sup>These authors contributed equally to this work.

factors from the circulation into the local tissue (4). C5a can be quickly degraded to C5a *desArg* by carboxypeptidases available abundantly in tissues and serum (5).

Translational research efforts support a positive role for C5a in anti-tumor monoclonal antibody (mAb) therapy. Yeast-derived  $\beta$ -glucan polysaccharide adjuvant therapy has been demonstrated to prime C receptor 3 (CR3) on neutrophils for enhanced tumor killing (6). C activation during  $\beta$ -glucan therapy is critical for efficacy, as it leads to the release of C5a responsible for recruiting  $\beta$ -glucan-primed neutrophils (7). Expression of CD55 by SKOV-3 inhibits the release of C5a thus limiting therapeutic efficacy of combined  $\beta$ -glucan with anti-Her2/neu Ab treatment *in vivo* (8). Additionally, *in vitro* studies involving human breast cancer cells demonstrated improvement in tumor cell killing by neutrophils following treatment of cells with anti-Her2/neu mAb fused to either C5a or C5a *desArg* (9). Furthermore, murine mammary sarcoma EMT6 cells transfected with mouse C5a, which were capable of producing low levels of C5a and inducing minimal migration of J774 macrophage cells *in vitro*, had the most substantial reduction in tumor growth and regression as compared to control EMT6 cells (10). Contrary to these findings, a more recent study demonstrated a pro-tumorigenic role of C5a generated via the classical pathway within the tumor microenvironment (11). In this TC-1 murine cervical cancer model, C5a was shown to recruit significantly more myeloid-derived suppressor cells (MDSCs) and enhance the production of immunosuppressive reactive oxygen species (ROS) and reactive nitrogen species (RNS) by these cells resulting in the inhibition of the anti-tumor specific CD8<sup>+</sup> T cell response and increased tumor burden (11). Thus, the role of C5a in the tumor remains controversial (12–14).

In the current study, we addressed the role of C5a on tumor growth by transfecting tumor cells with mouse C5a. We found that the local C5a concentration within the tumor microenvironment is critical in determining its role in tumor progression.

## Material and methods

### C5a transfection and mouse tumor models

Murine lymphoma RMA and human ovarian carcinoma SKOV-3 cells from the American Tissue Type Collection (ATCC, Manassas, VA) were transfected with secreting murine C5a or empty vector DNA plasmids generously provided by Dr. Fangting Liang at the Veterinary School of Medicine at Louisiana State University. Transfection using the Lipofectamine reagent (Invitrogen, Carlsbad, CA) was performed according to the manufactures guidelines. Supernatants from wells of confluent, G418 selected cells were screened by C5a ELISA (BD Biosciences, Bedford, MA) and also performed chemotaxis assay using murine macrophage J774 cells. Positively transfected cells, identified by ELISA were plated in a limiting dilution assay to isolate single clones expressing C5a for injection and were then passaged *in vivo* and following excision, re-screened by ELISA and immunohistochemistry for C5a expression. *In vitro* tumor cell growth rates were measured in real-time, using the ACEA system (Acea Biosciences, Inc.; San Diego, CA) as described previously (15). Each cell line was plated in quadruplicate in the ACEA 16-well plate. Cell index was recorded to reveal tumor cell growth.

All mice used for *in vivo* studies were approved and treated following requirements of the Institutional Animal Care and Use Committee (IACUC) of the University of Louisville. Studies were performed on both Severe Combined Immunodeficient (SCID) mice 6–10 weeks of age purchased from Taconic (Germantown, NY) or Harlan Laboratories (Fox Chase Cancer Center, PA) and wildtype C57Bl/6 mice (NCI, Frederick, MD). For SKOV-3 tumor model, 7–10 $\times$ 10<sup>6</sup> C5a-transfected or control vector (CV)-transfected SKOV-3 cells were injected subcutaneously (s.c.) with matrigel (BD Biosciences). For murine lymphoma

RMA model, female C57BL/6 mice were implanted s.c. with RMA-C5a (3CF4), RMA-C5a (1474), or RMA-CVA1 cells ( $2 \times 10^5$  per mouse). Tumor growth was monitored by caliper measurement.

### C5a ELISA

ELISA plates were coated with  $2\mu\text{g/mL}$  purified rat anti-mouse C5a mAb (BD Biosciences) for overnight at  $4^\circ\text{C}$ . Culture supernatants from transfected cells were added and the biotinylated rat anti-mouse C5a detection Ab (BD Biosciences) was applied at a concentration of  $2\mu\text{g/mL}$ . Assays were developed with tetramethylbenzidine (TMB) conductivity substrate (BioFX Laboratories, Inc., Owings Mills, MD) and the OD value was measured at 450 nm.

### Immunohistochemistry (IHC) and immunofluorescent (IF) staining

Frozen tumor tissue sections were fixed in ice-cold acetone. Appropriate blocking steps were performed on tissue samples including 3% hydrogen peroxide, 3% BSA in 1X PBS, and avidin/biotin blocking kit (Vector Laboratories, Inc. Burlingame, CA). Biotinylated rat anti-mouse C5a Ab (BD Biosciences) was added at  $2\mu\text{g/mL}$ . Slides were incubated in the humidity chamber overnight at  $4^\circ\text{C}$ . Streptavidin-HRP (Vector Laboratories) was prepared and applied to slides. Slides were rinsed and then incubated with the 3-amino-9-ethylcarbazole (AEC) substrate solution (Vector Laboratories). Slides were then counterstained with hematoxylin. Images were acquired with Aperio ScanScope digital scanners. For IF staining, slides were stained with DX5 Alexa Fluor 647 or F4/80 APC (Biolegend, San Diego, CA) with appropriate isotype controls. Slides were washed and 4'-6-Diamidino-2-phenylindole (DAPI, Invitrogen) nuclear stain was added. Images were acquired by Leica TCS SP5 confocal microscopy system.

### *In vitro* cytotoxicity

*In vitro* cytotoxicity assay was performed using the ACEA system as previously described (15). Several innate immune cell populations were used in various cytotoxicity experiments. Single cell suspensions prepared from naïve SCID mouse spleens were added to a flask and cultured briefly for macrophage adherence. Non-adherent cells that contained mostly NK cells and neutrophils were collected for cytotoxicity studies. These innate immune cells were added at an effector to tumor cell ratio of 20:1. To examine Gr-1<sup>+</sup>CD11b<sup>+</sup> myeloid cell inhibitory activity, Gr-1<sup>+</sup>CD11b<sup>+</sup> cells sorted from SKOV-3 C5a and SKOV-3 CV tumors were added to wells containing the growing SKOV-3 WT cells in the presence or absence of SCID mouse non-adherent leukocytes. NK cells were also purified from naïve SCID mouse spleens using the EasySep magnetic beads kit (StemCell Technologies, British Columbia, Canada). Percent of cytotoxicity was calculated as previously described (15).

### Flow cytometry

Excised tumor masses were minced and mixed with digestion buffer to prepare single cell suspensions. Cells from tumor, tumor-draining lymph nodes (TDLN), and spleen were blocked with CD16/32 Fc $\gamma$  receptor mAb. Surface marker staining on the prepared single cell suspensions was performed on ice. For intracellular staining, the cells were stimulated with PMA/ionomycin in the presence of Golgiplug for 4 hr. The staining was performed using Foxp3 staining buffer set (eBioscience or biolegend, San Diego, CA) according to the manufacturer's protocol. The following fluorochrome-conjugated mAbs were used: Gr-1, CD11b, F4/80, DX5, NK1.1, CD4, CD8, IFN- $\gamma$ , IL-17, and Foxp3 (Biolegend). Cells were collected on FACS Calibur followed by analysis using FloJo software (TreeStar, Ashland, OR).

### Quantitative real-time PCR (qRT-PCR)

Small portions of excised tumors were removed with a scalpel blade and weighed. Tumor tissues with similar weight were placed in 1mL of Trizol reagent (Invitrogen) and kept at  $-80^{\circ}\text{C}$ . Sorted cells were also placed in Trizol. RNAs were isolated using a Qiagen RNeasy kit according to the manufacturer's instructions (Qiagen, Valencia, CA). A set amount of RNA was also used to control for differences in tumor size. After reverse transcription into cDNA with a Reverse Transcription Kit (Bio-Rad, Hercules, CA), qRT-PCR was then performed on Bio-Rad MyiQ single color RT-PCR detection system using SYBR Green Supermix (Bio-Rad) and gene-specific primers summarized in the Supplemental Table I. Gene expression levels were normalized to glyceraldehyde 3-phosphate dehydrogenase (GAPDH) housekeeping gene and data was represented as fold differences by the  $2^{-\Delta\Delta\text{Ct}}$  method, where  $\Delta\text{Ct}=\text{Ct}_{\text{target gene}}-\text{Ct}_{\text{GAPDH}}$  and  $\Delta\Delta\text{Ct}=\Delta\text{Ct}_{\text{induced}}-\Delta\text{Ct}_{\text{reference}}$ .

### Cytospin and stain

Sorted cells were applied to the Shandon pre-made cuvettes (Shandon Inc, Pittsburg, PA) and slide, and spun in Shandon Cytospin 3 centrifuge. After spinning cells were fixed to the slide with methanol and stained with PROTOCOL Hema 3 solution I and II (Fisher Diagnostics, Middletown, VA). Cells were analyzed by microscopy under 20X and 40X magnification. Images were captured using the Nikon Eclipse E400.

### T cell differentiation assay

Naïve CD4 T cells from OT-II ovalbumin (OVA) TCR transgenic mice (Taconic) were purified by microbead separation (AutoMACS, Miltenyi Biotec). Macrophages were harvested from peritoneal cavity and purified with F4/80 microbeads. Macrophages were cultured with varying concentrations of C5a (R&D Systems) for 24 h and then co-cultured with CD4 T cells (2:1 ratio) in the presence of OVA (15  $\mu\text{g}/\text{ml}$ ) for additional 3 days. For Treg induction assay, macrophages were co-cultured with CD4 T cells in the presence of OVA and varying amounts of C5a for 4 days. Cells were re-stimulated with PMA/ionomycin in the presence of Golgiplug for 4 hr. Intracellular IFN- $\gamma$ , IL-17, or Foxp3 staining was performed.

### Graphing and statistical analysis

Prism 5.0 (GraphPad Software: San Diego, CA) was utilized in creating graphs and analyzing data collected from *in vitro* and *in vivo* studies. Following C5a ELISA the standard curve was graphed, linear regression test performed, and sample concentrations were extrapolated from the standard curve. Analysis of tumor growth significance and significance between the percentages of infiltrating cells or cytokine-secreting cells and qRT-PCR data analysis utilized the Student's t test or two-way ANOVA.

## Results

### C5a-expressing tumor cells have significantly reduced growth in SCID mice

The human ovarian adenocarcinoma cell line, SKOV-3, has been shown to overexpress the CRP CD55 (8). CD55 accelerated inhibition of C5a release and resulted in diminished tumor infiltration of  $\beta$ -glucan-primed neutrophils (8). To determine if C5a expression could enhance the recruitment of innate leukocytes to the tumor microenvironment, eliminating the negative effects of CD55, SKOV-3 cells were transfected with mouse C5a or CV. SKOV-3 WT cells were confirmed not to express C5a by ELISA and IHC while SKOV-3 C5a tumors had abundant C5a deposition (Supplemental Figure 1A). *In vitro* chemotaxis assay indicated supernatants from SKOV-3 C5a tumor cells enhanced migration of J774

cells (data not shown), suggesting that C5a secreted from transfected tumor cells was functionally active.

To determine whether the transfection of C5a introduced any growth disparities on cells, *in vitro* growth kinetics was monitored. Both C5a- and CV-transfected clones displayed an initial *in vitro* growth enhancement over SKOV-3 WT cells but no longer apparent after 12 hr of culture; all three cell lines were determined to grow equally well (Supplemental Figure 1B). Selected clones were then used to observe their *in vivo* tumor growth. Using the SCID-immunocompromised/SKOV-3 tumor model was beneficial on two fronts. It permitted for focus on the effect of C5a on innate leukocyte infiltration and functional activity of these cells in the tumor, exclusively, which were hypothesized to be the main targets. Additionally, the model allowed for study of an aggressive, human carcinoma which overexpresses CD55 (8) resulting in the inhibition of C activation at the C3 and C5 convertase step, eliminating local C5a release. All tumor cell lines demonstrated similar initial *in vivo* growth; however, beginning around day 24 post injection, SKOV-3 C5a tumors revealed significant reduction in tumor progression (Figure 1A). Upon excision at an endpoint time between 31 and 38 days for three separate experiments, C5a expressing tumors weighed significantly less than both CV and WT tumors (Figure 1B).

### Enhanced infiltration of innate immune cell subsets in SKOV-3 C5a-expressing tumors

Innate immune cells have been shown to be important to mount an anti-tumor response (7, 16, 17), as well as play an important role in sustaining the immunosuppressive environment and angiogenic switch promoting tumor growth and metastasis (18, 19). Expression of C5a from the tumor environment may harness the anti-tumor response of these cells. We found a slight increase in circulating DX5<sup>+</sup> NK cells from spleen and peripheral blood samples and a surprising decrease in splenic Gr-1<sup>+</sup> CD11b<sup>+</sup> cells compared to naïve SCID (data not shown). Tumors were then examined for the role of C5a in enhancing the migration of innate leukocytes into the tumor tissue. Flow cytometric analysis revealed that there was no difference in the percentage of Gr-1<sup>+</sup>CD11b<sup>+</sup> cells infiltrating the tumor (Figure 2A). However, C5a tumors showed an increased percentage of infiltrating DX5<sup>+</sup>CD11b<sup>+</sup> NK cells (Figure 2B) and F4/80<sup>+</sup>CD11b<sup>+</sup> subsets of macrophages (Figure 2C). Taken together, C5a appears to be enhancing the infiltration of NK cells and macrophages in tumor, two distinct subsets of innate immune cells that have been shown to be important in tumor immunity.

### Tumor microenvironment analysis reveals a significant decrease in the production of pro-tumorigenic factors

Next, we examined pro- and anti-tumorigenic gene levels to identify alterations in the tumor microenvironment as a result of C5a expression. When the total tumor samples were analyzed by qRT-PCR, many genes evaluated did not show a difference: inducible nitric oxide synthase (iNOS), transforming growth factor- $\beta$  (TGF- $\beta$ ), interleukin (IL) IL-6, IL-10, IL-12, IFN- $\gamma$ , granzyme B, or perforin (Figure 3A and data not shown). However, the mRNA levels of vascular endothelial growth factor (VEGF), arginase and tumor necrosis factor-alpha (TNF- $\alpha$ ) were significantly lower in C5a-expressing tumors (Figure 3A). To further delineate the source of VEGF and iNOS influenced by C5a, both CD11b<sup>+</sup> leukocytes and CD11b<sup>-</sup> tumor cells were analyzed (Figure 3B). This data indicated the activity of C5a in reduction of VEGF on tumor cells. In contrast, iNOS mRNA level was significantly lower in C5a-expressing SKOV-3 tumor-infiltrating leukocytes (Figure 3B). Isolation of F4/80<sup>+</sup> infiltrates followed by qRT-PCR demonstrated no difference in the case of VEGF, iNOS, TNF- $\alpha$  or IL-12 (data not shown); however, F4/80<sup>+</sup> cells infiltrating SKOV-3 C5a tumors made significantly less arginase (Figure 3C), suggesting an anti-tumor macrophage phenotype.

### The presence of C5a renders naïve innate leukocytes more cytotoxic to tumor cells and decreases Gr-1<sup>+</sup>CD11b<sup>+</sup> cell inhibitory activity

*In vitro* studies were enlisted to determine whether C5a could enhance the cytotoxicity of tumor cells by naïve innate leukocytes. Compared to SKOV-3 CV cells, SKOV-3 C5a cells were killed at a significantly higher percent by the naïve leukocytes (Figure 4A). In addition, NK cells from naïve mouse had significantly higher killing activity for SKOV-3 C5a tumor cells as compared to SKOV-3 CV cells (Figure 4B). These results indicate C5a has activating potential of naïve neutrophils and/or NK cells for superior effector function.

As shown in Figure 2A, the frequency of Gr-1<sup>+</sup>CD11b<sup>+</sup> cells was not significantly altered in C5a expressing tumor. Next, we examined the inhibitory activity of tumor-infiltrating Gr-1<sup>+</sup>CD11b<sup>+</sup> cells on naïve, non-adherent leukocytes-mediated cytotoxicity of tumor cells. Non-adherent leukocytes from naïve SCID mice showed significant level of cytotoxicity against SKOV-3 tumor cells. The Addition of Gr-1<sup>+</sup>CD11b<sup>+</sup> cells from either SKOV-3 C5a or SKOV-3 CV tumors significantly inhibited cytotoxic activity (Figure 4C). However, Gr-1<sup>+</sup>CD11b<sup>+</sup> cells from SKOV-3 C5a tumors were significantly less suppressive. In the absence of the naïve leukocytes, neither tumor isolated Gr-1<sup>+</sup>CD11b<sup>+</sup> cells led to SKOV-3 WT tumor cell destruction. They actually promoted tumor cell growth *in vitro*. The images of the Gr-1<sup>+</sup>CD11b<sup>+</sup> cells demonstrated nearly all these cells were morphologically similar to neutrophils (Figure 4D).

### C5a-expressing tumor cells have significantly accelerated growth in immunocompetent mice

Although the SCID mouse model allows us to study C5a effect on innate immune cells, these mice lack adaptive T/B cells. To determine C5a-expressing tumor growth in immunocompetent host, murine lymphoma RMA cells with or without C5a expression were implanted in wildtype C57Bl/6 mice. Surprisingly, C5a-expressing tumors (RMA-3CF4) grew significantly faster than CV-transfected cells (RMA-CVA1) from all three independent experiments (Figure 5A and data not shown). The frequency of Gr-1<sup>+</sup>CD11b<sup>+</sup> MDSCs was significantly higher in RMA-3CF4 spleen compared to RMA-CVA1 although no difference was observed in TDLN and tumors (Figure 5B). Innate immune cells including F4/80<sup>+</sup> macrophages and NK1.1<sup>+</sup> NK cells were largely unchanged (Figure 5B).

Strikingly, the frequency of both CD4<sup>+</sup> and CD8<sup>+</sup> T cells from spleen, TDLN, and tumor was significantly lower in C5a-expressing tumor-bearing mice as compared to CV tumor-bearing mice (Figure 5C and D). However, significantly more of the RMA-3CF4 spleen and TDLN infiltrating CD8<sup>+</sup> T cells produced IFN- $\gamma$ , although a similar percentage of IFN- $\gamma$ -producing CD8<sup>+</sup> T cells was observed in tumor. In addition, the percentage of CD4<sup>+</sup> T cells from RMA-3CF4 spleen and tumor producing IFN- $\gamma$  displayed a slightly different pattern. Significantly more of the splenic CD4<sup>+</sup> T cells produced IFN- $\gamma$ , however, significantly less tumor-infiltrating CD4<sup>+</sup> T cells produced IFN- $\gamma$  when compared to CVA1 controls. In addition, splenic regulatory T cells (Treg) were significantly increased in C5a-expressing tumor-bearing mice (Supplemental Figure 2A) as compared to CVA1 animals. Taken together, RMA-3CF4 tumor-bearing mice had overall significantly lower percentages of infiltrating CD4<sup>+</sup> and CD8<sup>+</sup> T cells in spleen, TDLN, and tumor, with an increased percentage of these subsets producing IFN- $\gamma$  in the spleen and TDLN by CD8<sup>+</sup> T cells and in the spleen by CD4<sup>+</sup> T cells but decreased IFN- $\gamma$  production by tumor-infiltrating CD4<sup>+</sup> T cells.

### Low C5a production from tumor cells significantly decreases tumor growth

Given the contradictory data generated from the different models, we noted C5a concentrations detected from SKOV-3 versus RMA cells differed. RMA-3CF4 cells secreted

higher levels of C5a as compared to SKOV-3 C5a cells (data not shown). Next we examined whether C5a levels from tumor cells have any impact on the tumor growth. As shown in Figure 6A, RMA1474 cells secreted low level of C5a, which is comparable to SKOV-3 C5a. These cells had significantly delayed tumor progression as compared to RMA-CVA1 (Figure 6B), similar to the SKOV-3 model.

In contrast to RMA-3CF4 tumor, Gr-1<sup>+</sup>CD11b<sup>+</sup> MDSC frequency was not significantly changed between RMA-CVA1 and RMA-1474 tumor-bearing mice (Figure 6C). T cell infiltration patterns also differed between the groups of RMA tumors. Percentages of infiltrating CD4<sup>+</sup> and CD8<sup>+</sup> T cells were significantly increased in spleen but significantly decreased in TDLN in RMA-1474 tumor-bearing mice. In addition, splenic Treg was comparable in RMA-1474 versus CVA1 tumor-bearing mice (Supplemental Figure 2B). While there were significantly fewer of the T cell subsets infiltrating RMA-3CF4 tumors with high levels of C5a, no difference was observed in the percentage of infiltration of tumors between CVA1 and RMA-1474 with low C5a (Figure 6D and E). Similar to RMA-3CF4 T cell populations, a significantly greater percentage of CD4<sup>+</sup> and CD8<sup>+</sup> T cells produced IFN- $\gamma$  in spleen and TDLN of RMA-1474 tumor bearing mice.

### C5a drives Th1 and Treg differentiation via concentration-dependent manner

C5a has been previously demonstrated to stimulate Th17 cell differentiation and trigger autoimmune arthritis and experimental autoimmune encephalomyelitis (20, 21). We next examined whether Th cell differentiation mediated by C5a was also concentration dependent. To this end, naive OVA TCR transgenic CD4 T cells were cultured with macrophages in the presence of varying levels of C5a. As shown in Figure 7A, C5a at the concentrations of 100 ng/ml and 300 ng/ml significantly promoted Th1 cell differentiation as revealed by more IFN- $\gamma$  production. However, C5a at the higher level (500 ng/ml) significantly decreased Th1 (Figure 7A). In contrast, low concentrations of C5a gradually decreased Treg induction (Figure 7C). C5a at 100 ng/ml and 300 ng/ml significantly decreased Treg induction while C5a was at the higher concentration significantly promoted Treg induction (Figure 7C). These effects were completely abrogated in C5aR-deficient mice (data not shown). No difference was observed for Th17 cell differentiation (Figure 7B). These data suggest that C5a-mediated Th1 and Treg differentiation appear to be bell-shaped.

## Discussion

Thus far, the role of C5a in the tumor microenvironment has been inconclusive, with previously published studies demonstrating either C5a release from the tumor resulted in reduced tumor growth (10) or C5a enhanced immune suppressive cells and supported tumor growth (11). We have demonstrated here in the SKOV-3 xenograft model support of a pro-immunogenic, anti-tumor role for C5a released in the tumor microenvironment. C5a is acting on host immune cells and indirectly on tumor cells to alter the cytokine milieu and enhance tumor infiltration and cytotoxic function of innate immune effector cells. The C5a effect in the immunocompetent model appears to be concentration dependent. High C5a levels stimulate tumor growth with significantly decreased infiltration of CD4<sup>+</sup> and CD8<sup>+</sup> T cells while low levels of C5a within the tumor microenvironment decrease tumor progression. Therefore, local C5a concentration is critical in determining its role in tumor progression.

In the SKOV-3 xenograft model, the effect of C5a release in the tumor elicits minimal changes in the periphery and dramatic changes occur in the tumor microenvironment. Since SKOV-3 tumor cells lack C5aR expression, the reduced *in vivo* growth of SKOV-3 tumor cells expressing C5a is likely due to the responses by host innate immune cells. As

demonstrated by the *in vitro* cytotoxicity assay, the C5a secreted from tumor cells enhances the effector functions of neutrophils and NK cells *in vitro* and renders them more cytotoxic to the tumor cells. Similarly, a recent study showed that C5a-C5aR interaction enhanced NK cell IFN- $\gamma$  production in sepsis (22). C5a release in the tumor also enhances the recruitment of innate immune cells to the tumor. Enhanced recruitment of the DX5<sup>+</sup>CD11b<sup>+</sup> NK cells into the tumor is beneficial because of the tumor cytotoxic and immune enhancing potential of NK cells (23, 24). In solid tumors, NK cell penetration is noted as a positive prognostic factor, but most solid tumors demonstrate inferior NK cell infiltration (23). In C5a-expressing tumor, macrophages are also significantly increased. Macrophages play a dominant role in influencing other immune cells and tumor growth depending on phenotype (25, 26). Two extreme ends of macrophage polarization have been characterized based on the stimulatory factors and products released by the cells: M1 (anti-tumorigenic) and M2 (pro-tumorigenic) macrophages (25, 27). As shown in the current study, macrophages from C5a-expressing tumor have significantly low mRNA levels of arginase, suggesting an M1 phenotype. Although the frequency of Gr-1<sup>+</sup>CD11b<sup>+</sup> cells is similar in SKOV3 C5a and SKOV-3 CV tumor, the abundant expression of C5aR on these cells renders them most sensitive to local C5a concentrations. Indeed, Gr-1<sup>+</sup>CD11b<sup>+</sup> cells from SKOV-3 C5a tumor have less immune suppressive effect as compared to those from SKOV-3 CV tumor. Thus local C5a may promote innate immune cell traffic into tumor, and once immune cells are recruited, C5a can activate and enhance the cytotoxic functions.

C5a also leads to events that can alter a local tumor environment. Significant changes in four important tumor and immune regulating factors exist between SKOV-3 C5a and SKOV-3 CV tumors: arginase, iNOS, VEGF, and TNF- $\alpha$ . Arginase and iNOS are essential for MDSC-mediated immune suppressive effect (28, 29). VEGF and its role in angiogenesis and tumor neovascularization are exploited by the tumor (30) (31, 32). We show that it is the tumor cells and not the immune infiltrating CD11b<sup>+</sup> cells that express significantly more VEGF. Due to the lack of C5aR expression on tumor cells, the mechanism of C5a is indirect. A recent study also demonstrated that C5a negatively regulates neovascularization and angiogenesis via secretion of soluble VEGF receptor 1 (sVEGFR1) (33).

On the contrary, C5a-expressing tumor cells in immunocompetent mice showed more complexing results. High C5a release in the tumor microenvironment promotes tumor progression, which is similar as TC-1 tumor model (11). The most striking finding from this model is the overall decreased frequencies of CD4<sup>+</sup> and CD8<sup>+</sup> T cells in spleen, TDLN and tumor in high C5a-expressing tumor-bearing mice. While MDSCs significantly accumulated in spleen. MDSCs have been shown to down-regulate L-selectin expression on CD4<sup>+</sup> and CD8<sup>+</sup> T cells thus decreasing their homing to sites where they should be activated (34, 35). The decreased CD4<sup>+</sup> and CD8<sup>+</sup> T cells in C5a high expressing tumor-bearing mice could be due to the accumulated MDSCs in spleen. This is also supported by the data generated from low C5a expressing tumor where MDSCs are not significantly altered and CD4<sup>+</sup> and CD8<sup>+</sup> T cells are increased in spleen and decreased in TDLN but equivalent in tumor. The C system has recently demonstrated to be critical in regulating adaptive T cell responses (36). C activation can regulate CD4<sup>+</sup> Th1, Treg, and Th17 cell differentiation (20, 21, 37–40) as well as CD8<sup>+</sup> T cell immunity (41, 42). Indeed, IFN- $\gamma$ -producing CD8<sup>+</sup> T cells are significantly increased in spleen and TDLN in both high and low C5a expressing tumor-bearing mice, suggesting C5a can augment IFN- $\gamma$  production by CD8<sup>+</sup> T cells at distant sites. However, IFN- $\gamma$ -producing CD4<sup>+</sup> T cells are differentially regulated by C5a as tumor-infiltrating IFN- $\gamma$ -producing CD4<sup>+</sup> T cells are significantly decreased in high C5a expressing tumor while no difference is observed in C5a low expressing tumor. This is further supported by the *in vitro* CD4<sup>+</sup> T cell differentiation experiments showing C5a at 100 ng/ml and 300 ng/ml promotes Th1 responses while C5a at the higher concentration (500 ng/ml) inhibits Th1 and promotes Treg differentiation. In addition, splenic Treg cells

are significantly increased in C5a high tumor-bearing mice while are comparable in C5a low tumor-bearing animals as compared to CV tumor-bearing mice.

We thus hypothesize that tumor growth outcomes may differ tremendously due to C5a concentration levels in the local tumor microenvironment. High C5a levels may lead to either over-activation of infiltrating cells or enhancement of an inflammatory setting to perpetuate tumor growth, angiogenesis, and suppression of the anti-tumor T cell infiltration. This may be analogous to the sepsis during which an over-activated C system, *e.g.* the release of high levels of C5a, disables innate immune cells, decreasing phagocytic function and resulting in an overall immunosuppressive state (43). Conversely, low levels of the C protein may enhance infiltration of immune cells, and upon entry into the environment, C5a at low levels stimulates a more powerful anti-tumor immune response. However, quantitation of the chemoattractant C5a and its quick degradation by enzymes in the environment complicate pinpointing the critical concentration threshold of C5a. This is particularly important in the setting of *in vivo* anti-tumor mAb therapy. In addition, the C5a levels could be very different in the current model system where tumors continuously secrete C5a while under natural condition C5a is primarily produced through local complement fixation. More work needs to be done to determine whether the current findings are relevant for an *in vivo* immunotherapeutic setting. In addition, the differences observed in the two model systems need to be reconciled due to different tumor types, mouse strains and the presence or absence of adaptive immune system. Nevertheless, the evidence generated from previous studies (10, 11) and the current work support the hypothesis that C5a concentration holds the key to the response generated to tumor.

## Supplementary Material

Refer to Web version on PubMed Central for supplementary material.

## Acknowledgments

This study was supported by research funding from NIH R01 CA86412, R01 CA150947 and the Kentucky Lung Cancer Research Board (JY).

## References

1. Huber-Lang M, Sarma JV, Zetoune FS, Rittirsch D, Neff TA, McGuire SR, Lambris JD, Warner RL, Flierl MA, Hoesel LM, Gebhard F, Younger JG, Drouin SM, Wetsel RA, Ward PA. Generation of C5a in the absence of C3: a new complement activation pathway. *Nat Med.* 2006; 12:682–687. [PubMed: 16715088]
2. Spendlove I, Ramage JM, Bradley R, Harris C, Durrant LG. Complement decay accelerating factor (DAF)/CD55 in cancer. *Cancer Immunol Immunother.* 2006; 55:987–995. [PubMed: 16485129]
3. Yan J, Allendorf DJ, Li B, Yan R, Hansen R, Donev R. The role of membrane complement regulatory proteins in cancer immunotherapy. *Advances in experimental medicine and biology.* 2008; 632:159–174. [PubMed: 19025121]
4. Guo RF, Ward PA. Role of C5a in inflammatory responses. *Annu Rev Immunol.* 2005; 23:821–852. [PubMed: 15771587]
5. Ehrnthaller C, Ignatius A, Gebhard F, Huber-Lang M. New insights of an old defense system: structure, function, and clinical relevance of the complement system. *Mol Med.* 2011; 17:317–329. [PubMed: 21046060]
6. Liu J, Gunn L, Hansen R, Yan J. Combined yeast-derived beta-glucan with anti-tumor monoclonal antibody for cancer immunotherapy. *Exp Mol Pathol.* 2009; 86:208–214. [PubMed: 19454271]
7. Allendorf DJ, Yan J, Ross GD, Hansen RD, Baran JT, Subbarao K, Wang L, Haribabu B. C5a-Mediated Leukotriene B4-Amplified Neutrophil Chemotaxis Is Essential in Tumor Immunotherapy

- Facilitated by Anti-Tumor Monoclonal Antibody and  $\beta$ -Glucan. *J Immunol.* 2005; 174:7050–7056. [PubMed: 15905548]
8. Li B, Allendorf DJ, Hansen R, Marroquin J, Cramer DE, Harris CL, Yan J. Combined yeast  $\beta$ -glucan and antitumor monoclonal antibody therapy requires C5a-mediated neutrophil chemotaxis via regulation of decay-accelerating factor CD55. *Cancer Res.* 2007; 67:7421–7430. [PubMed: 17671212]
  9. Fuenmayor J, Perez-Vazquez K, Perez-Witzke D, Penichet ML, Montano RF. Decreased survival of human breast cancer cells expressing HER2/neu on in vitro incubation with an anti-HER2/neu antibody fused to C5a or C5a desArg. *Molecular cancer therapeutics.* 2010; 9:2175–2185. [PubMed: 20682652]
  10. Kim DY, Martin CB, Lee SN, Martin BK. Expression of complement protein C5a in a murine mammary cancer model: tumor regression by interference with the cell cycle. *Cancer Immunol Immunother.* 2005; 54:1026–1037. [PubMed: 15868168]
  11. Markiewski MM, DeAngelis RA, Benencia F, Ricklin-Lichtsteiner SK, Koutoulaki A, Gerard C, Coukos G, Lambris JD. Modulation of the antitumor immune response by complement. *Nat Immunol.* 2008; 9:1225–1235. [PubMed: 18820683]
  12. Markiewski MM, Lambris JD. Unwelcome complement. *Cancer Res.* 2009; 69:6367–6370. [PubMed: 19654288]
  13. Markiewski MM, Lambris JD. Is complement good or bad for cancer patients? A new perspective on an old dilemma. *Trends Immunol.* 2009; 30:286–292. [PubMed: 19428302]
  14. Ostrand-Rosenberg S. Cancer and complement. *Nature biotechnology.* 2008; 26:1348–1349.
  15. Li B, Allendorf DJ, Hansen R, Marroquin J, Ding C, Cramer DE, Yan J. Yeast  $\beta$ -glucan amplifies phagocyte killing of iC3b-opsonized tumor cells via complement receptor 3-Syk-phosphatidylinositol 3-kinase pathway. *J Immunol.* 2006; 177:1661–1669. [PubMed: 16849475]
  16. Hicks AM, Riedlinger G, Willingham MC, Alexander-Miller MA, Von Kap-Herr C, Pettenati MJ, Sanders AM, Weir HM, Du W, Kim J, Simpson AJ, Old LJ, Cui Z. Transferable anticancer innate immunity in spontaneous regression/complete resistance mice. *Proc Natl Acad Sci U S A.* 2006; 103:7753–7758. [PubMed: 16682640]
  17. Nausch N, Cerwenka A. NKG2D ligands in tumor immunity. *Oncogene.* 2008; 27:5944–5958. [PubMed: 18836475]
  18. Nozawa H, Chiu C, Hanahan D. Infiltrating neutrophils mediate the initial angiogenic switch in a mouse model of multistage carcinogenesis. *Proc Natl Acad Sci U S A.* 2006; 103:12493–12498. [PubMed: 16891410]
  19. Qian BZ, Li J, Zhang H, Kitamura T, Zhang J, Campion LR, Kaiser EA, Snyder LA, Pollard JW. CCL2 recruits inflammatory monocytes to facilitate breast-tumour metastasis. *Nature.* 2011; 475:222–225. [PubMed: 21654748]
  20. Hashimoto M, Hirota K, Yoshitomi H, Maeda S, Teradaira S, Akizuki S, Prieto-Martin P, Nomura T, Sakaguchi N, Kohl J, Heyman B, Takahashi M, Fujita T, Mimori T, Sakaguchi S. Complement drives Th17 cell differentiation and triggers autoimmune arthritis. *J Exp Med.* 2010; 207:1135–1143. [PubMed: 20457757]
  21. Fang C, Zhang X, Miwa T, Song WC. Complement promotes the development of inflammatory T-helper 17 cells through synergistic interaction with Toll-like receptor signaling and interleukin-6 production. *Blood.* 2009; 114:1005–1015. [PubMed: 19491392]
  22. Fusakio ME, Mohammed JP, Laumonier Y, Hoebe K, Kohl J, Mattner J. C5a regulates NKT and NK cell functions in sepsis. *J Immunol.* 2011; 187:5805–5812. [PubMed: 22058413]
  23. Chan CJ, Andrews DM, Smyth MJ. Can NK cells be a therapeutic target in human cancer? *Eur J Immunol.* 2008; 38:2964–2968. [PubMed: 18979512]
  24. Smyth MJ, Hayakawa Y, Takeda K, Yagita H. New aspects of natural-killer-cell surveillance and therapy of cancer. *Nat Rev Cancer.* 2002; 2:850–861. [PubMed: 12415255]
  25. Qian BZ, Pollard JW. Macrophage diversity enhances tumor progression and metastasis. *Cell.* 2010; 141:39–51. [PubMed: 20371344]
  26. Ma J, Liu L, Che G, Yu N, Dai F, You Z. The M1 form of tumor-associated macrophages in non-small cell lung cancer is positively associated with survival time. *BMC cancer.* 2010; 10:112. [PubMed: 20338029]

27. Solinas G, Schiarea S, Liguori M, Fabbri M, Pesce S, Zammataro L, Pasqualini F, Nebuloni M, Chiabrando C, Mantovani A, Allavena P. Tumor-conditioned macrophages secrete migration-stimulating factor: a new marker for M2-polarization, influencing tumor cell motility. *J Immunol.* 2010; 185:642–652. [PubMed: 20530259]
28. Gabrilovich DI, Nagaraj S. Myeloid-derived suppressor cells as regulators of the immune system. *Nat Rev Immunol.* 2009; 9:162–174. [PubMed: 19197294]
29. Corzo CA, Condamine T, Lu L, Cotter MJ, Youn JI, Cheng P, Cho HI, Celis E, Quiceno DG, Padhya T, McCaffrey TV, McCaffrey JC, Gabrilovich DI. HIF-1 $\alpha$  regulates function and differentiation of myeloid-derived suppressor cells in the tumor microenvironment. *J Exp Med.* 2010; 207:2439–2453. [PubMed: 20876310]
30. Hanahan D, Weinberg RA. The hallmarks of cancer. *Cell.* 2000; 100:57–70. [PubMed: 10647931]
31. Chen W, Tang T, Eastham-Anderson J, Dunlap D, Alicke B, Nannini M, Gould S, Yauch R, Modrusan Z, DuPree KJ, Darbonne WC, Plowman G, de Sauvage FJ, Callahan CA. Canonical hedgehog signaling augments tumor angiogenesis by induction of VEGF-A in stromal perivascular cells. *Proc Natl Acad Sci U S A.* 2011; 108:9589–9594. [PubMed: 21597001]
32. Liu Y, Han ZP, Zhang SS, Jing YY, Bu XX, Wang CY, Sun K, Jiang GC, Zhao X, Li R, Gao L, Zhao QD, Wu MC, Wei LX. Effects of inflammatory factors on mesenchymal stem cells and their role in the promotion of tumor angiogenesis in colon cancer. *J Biol Chem.* 2011; 286:25007–25015. [PubMed: 21592963]
33. Langer HF, Chung KJ, Orlova VV, Choi EY, Kaul S, Kruhlak MJ, Alatsianos M, Deangelis RA, Roche PA, Magotti P, Li X, Economopoulou M, Rafail S, Lambris JD, Chavakis T. Complement-mediated inhibition of neovascularization reveals a point of convergence between innate immunity and angiogenesis. *Blood.* 2010; 116:4395–4403. [PubMed: 20625009]
34. Hanson EM V, Clements K, Sinha P, Ilkovich D, Ostrand-Rosenberg S. Myeloid-derived suppressor cells down-regulate L-selectin expression on CD4<sup>+</sup> and CD8<sup>+</sup> T cells. *J Immunol.* 2009; 183:937–944. [PubMed: 19553533]
35. Ostrand-Rosenberg S. Myeloid-derived suppressor cells: more mechanisms for inhibiting antitumor immunity. *Cancer Immunol Immunother.* 2010; 59:1593–1600. [PubMed: 20414655]
36. Carroll MC. The complement system in regulation of adaptive immunity. *Nat Immunol.* 2004; 5:981–986. [PubMed: 15454921]
37. Peng Q, Li K, Patel H, Sacks SH, Zhou W. Dendritic cell synthesis of C3 is required for full T cell activation and development of a Th1 phenotype. *J Immunol.* 2006; 176:3330–3341. [PubMed: 16517700]
38. Strainic MG, Liu J, Huang D, An F, Lalli PN, Muqim N, Shapiro VS, Dubyak GR, Heeger PS, Medof ME. Locally produced complement fragments C5a and C3a provide both costimulatory and survival signals to naive CD4<sup>+</sup> T cells. *Immunity.* 2008; 28:425–435. [PubMed: 18328742]
39. Lalli PN, Strainic MG, Yang M, Lin F, Medof ME, Heeger PS. Locally produced C5a binds to T cell-expressed C5aR to enhance effector T-cell expansion by limiting antigen-induced apoptosis. *Blood.* 2008; 112:1759–1766. [PubMed: 18567839]
40. Weaver DJ Jr, Reis ES, Pandey MK, Kohl G, Harris N, Gerard C, Kohl J. C5a receptor-deficient dendritic cells promote induction of Treg and Th17 cells. *Eur J Immunol.* 2010; 40:710–721. [PubMed: 20017191]
41. Fang C, Miwa T, Shen H, Song WC. Complement-dependent enhancement of CD8<sup>+</sup> T cell immunity to lymphocytic choriomeningitis virus infection in decay-accelerating factor-deficient mice. *J Immunol.* 2007; 179:3178–3186. [PubMed: 17709533]
42. Raedler H, Yang M, Lalli PN, Medof ME, Heeger PS. Primed CD8(+) T-cell responses to allogeneic endothelial cells are controlled by local complement activation. *American journal of transplantation : official journal of the American Society of Transplantation and the American Society of Transplant Surgeons.* 2009; 9:1784–1795. [PubMed: 19563342]
43. Ward PA. The dark side of C5a in sepsis. *Nat Rev Immunol.* 2004; 4:133–142. [PubMed: 15040586]

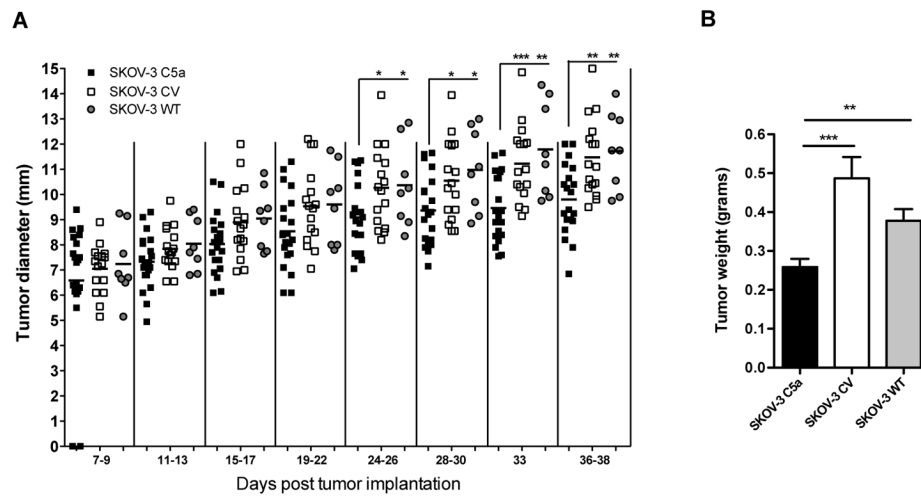


**Figure 1. *In vivo* growth of SKOV-3 tumor cells in SCID mice**

(A) *In vivo* growth of SKOV-3 C5a and controls revealed a significant reduction in tumor growth of SKOV-3 C5a. Following s.c. injection of SCID mice with SKOV-3 tumor cell lines (n=20, 16, 8 for SKOV-3 C5a, CV, WT; respectively), tumor growth was monitored by measuring two perpendicular diameters every 2–4 days. \*p<0.05, \*\*p<0.01, \*\*\*p<0.001. (B) Tumor weight measurement when all animals were sacrificed. \*\*p<0.01, \*\*\*p<0.001.

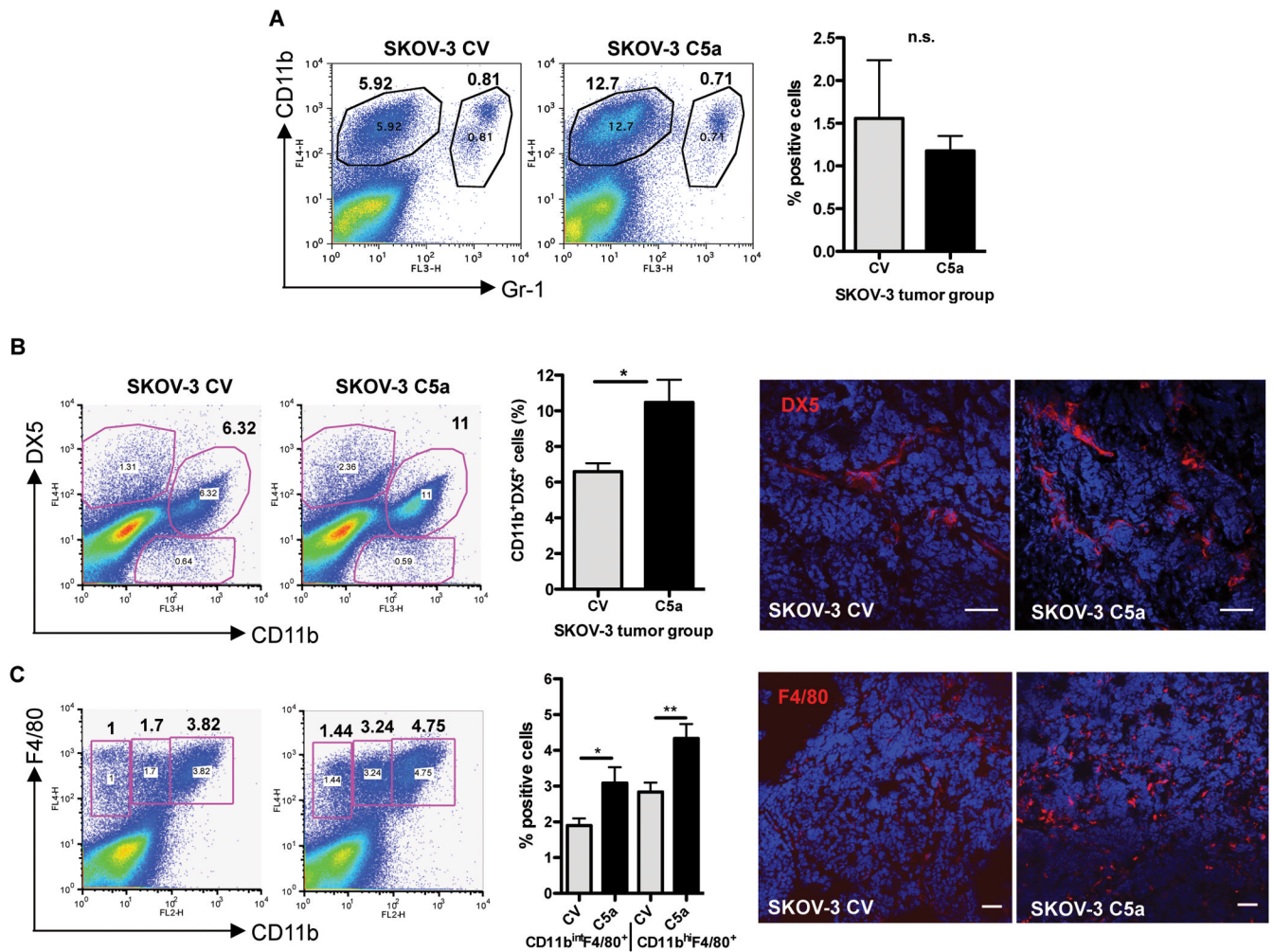


**Figure 2. Enhanced innate immune cell infiltration in SKOV-3 cells expressing C5a**  
 (A) Percentage of Gr-1<sup>+</sup>CD11b<sup>+</sup> cells in SKOV-3 C5a tumor and SKOV-3 CV tumor was not significantly altered. (B) Increased percentage of DX5<sup>+</sup>CD11b<sup>+</sup> NK cells were found to infiltrate SKOV-3 C5a tumors *in vivo*, as seen by flow cytometry and IF staining. \**p*<0.05. (C) Increased percentage of F4/80<sup>+</sup>CD11b<sup>+</sup> macrophages in SKOV-3 C5a tumors as determined by flow cytometry and IF staining. \**p*<0.05, \*\**p*<0.01. Representative data from SKOV-3 C5a (n=10) and SKOV-3 CV (n=9) tumors are shown. Bar, 50  $\mu$ m.

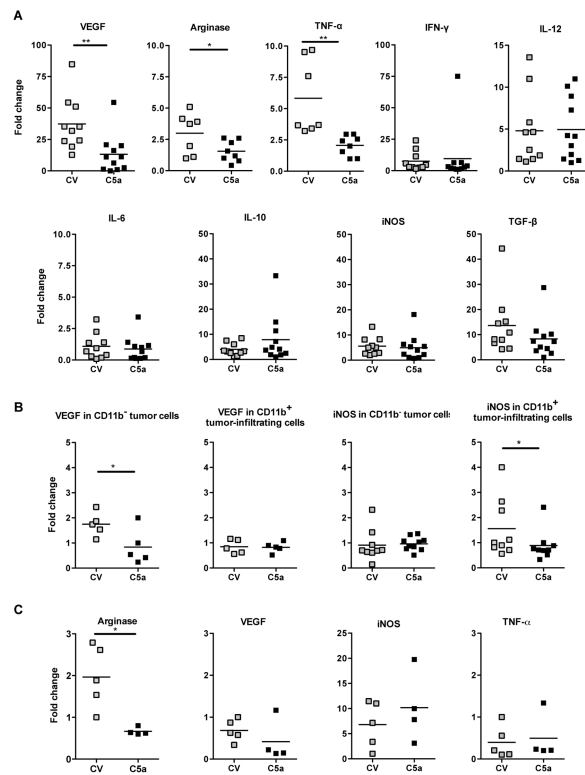


### Figure 3. The altered tumor microenvironment by C5a

(A) Total tumor samples were collected and RNAs were extracted. qRT-PCR data revealed the downregulation of VEGF, arginase, and TNF- $\alpha$  mRNA levels in C5a expressing tumors. \* $p < 0.05$ , \*\* $p < 0.01$ . (B) Sorted CD11b<sup>+</sup> innate immune cells and CD11b<sup>-</sup> tumor cells were performed for qRT-PCR analysis. Data indicate that VEGF mRNA level is significantly decreased in C5a expressing tumor cells while the CD11b<sup>+</sup> cells sorted from SKOV-3 C5a have significantly lower levels of iNOS mRNA. \* $p < 0.05$  (C) The SKOV-3 C5a infiltrating F4/80<sup>+</sup> macrophages expressed significantly lower levels of arginase mRNA. \* $p < 0.05$ .

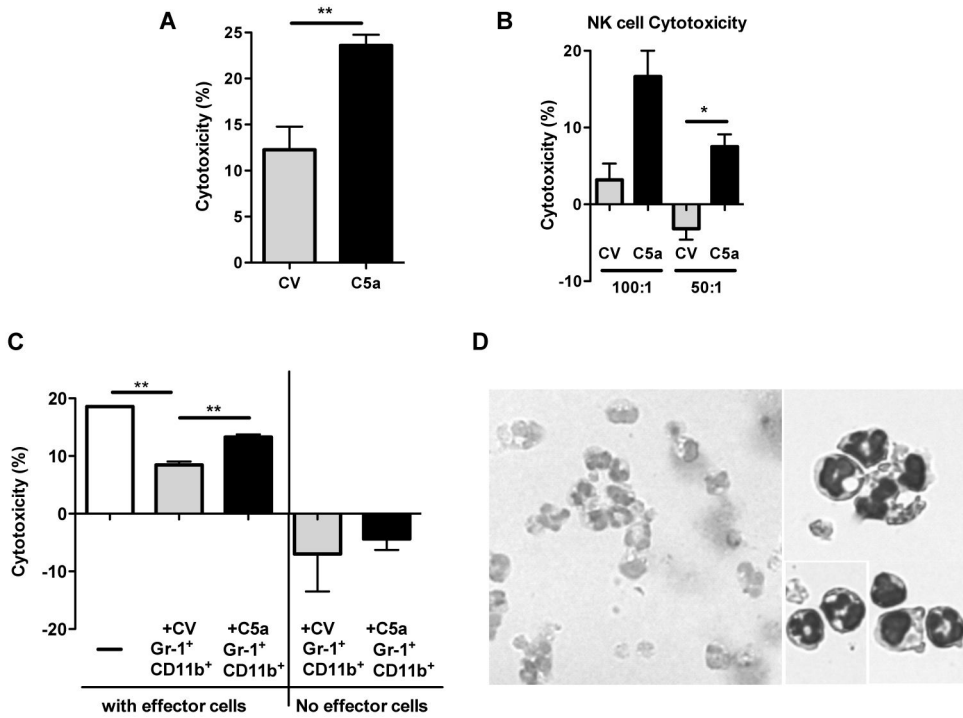


**Figure 4. C5a promotes cytotoxicity of SKOV-3 tumor cells while Gr-1<sup>+</sup>CD11b<sup>+</sup> cells from SKOV-3 C5a tumors are significantly less immunosuppressive**  
 (A) SKOV-3 C5a and CV tumor cells were cultured overnight, and the following day non-adherent leukocytes from naïve SCID mice as effector cells were added at a ratio of 20:1 (E:T). After 16 hours of co-culture, percent of cytotoxicity was calculated (n=6). Data indicate that effector cells kill significantly more SKOV-3 C5a cells than SKOV-3 CV cells. \*\*p<0.01. (B) Similarly, purified NK cells from naïve SCID mice were added to SKOV-3 C5a or CV tumor cells *in vitro*, and percent of cytotoxicity was determined following 24 hr co-culture. \*p<0.05. (C) SKOV-3 tumor cells were co-cultured with non-adherent leukocytes as effector cells (20:1) in the presence or absence of Gr-1<sup>+</sup>CD11b<sup>+</sup> cells sorted from CV or C5a-transfected tumor (1:1), or without effectors but with sorted Gr-1<sup>+</sup>CD11b<sup>+</sup> cells from tumor. The innate leukocytes demonstrated effective cytotoxicity of SKOV-3 tumor cells and cytotoxicity was significantly decreased in the presence of Gr-1<sup>+</sup>CD11b<sup>+</sup> cells sorted from tumors. However, Gr-1<sup>+</sup>CD11b<sup>+</sup> cells from SKOV-3 C5a tumors were significantly less suppressive. \*\*p<0.01. (D) Cytospin and stain of the Gr-1<sup>+</sup>CD11b<sup>+</sup> cells sorted from the SKOV-3 tumors. Images were acquired at 20X and 40X magnification.

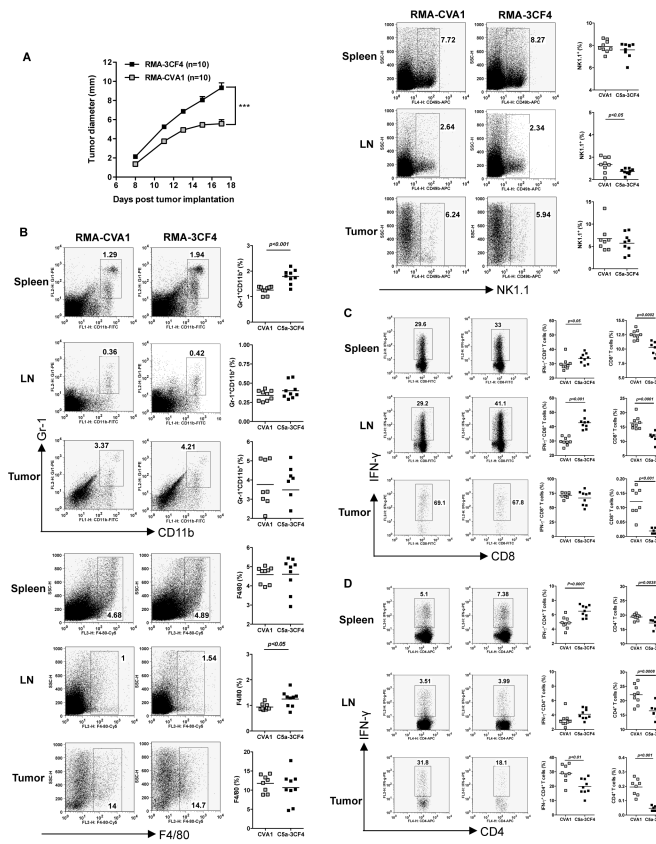


**Figure 5. C5a-expressing lymphoma cells have significantly enhanced tumor progression** (A) Wildtype C57Bl/6 mice were injected with C5a-expressing lymphoma RMA-3CF4 cells or RMA CVA1 cells (n=10) and tumor growth was recorded. Data are shown as mean ±s.e.m. \*\*\*p<0.001. (B) Spleen, TDLN, and tumor from tumor-bearing mice were prepared for single cell suspensions. Cells were then stained with Gr-1, CD11b, F4/80, or NK1.1. Representative dot plots and summarized data are shown. (C) Cells were stimulated with PMA/ionomycin and surface stained with CD8 and IFN-γ intracellularly. Representative dot plots (cells were gated on the CD8<sup>+</sup> T cells), summarized IFN-γ-producing CD8<sup>+</sup> T cells, and total CD8<sup>+</sup> T cells are shown. (D) Cells were stimulated with PMA/ionomycin and surface stained with CD4 and IFN-γ intracellularly. Representative dot plots (cells were gated on the CD4<sup>+</sup> T cells), summarized IFN-γ-producing CD4<sup>+</sup> T cells, and total CD4<sup>+</sup> T cells are shown.

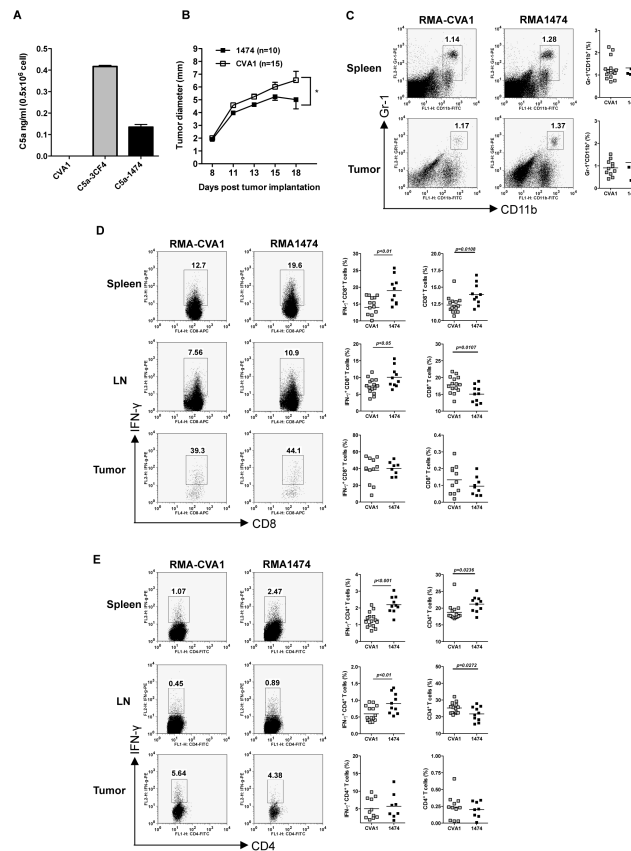


**Figure 6. Low C5a-expressing lymphoma cells have significantly decreased tumor progression** (A) C5a levels of RMA cells transfected with C5a or CV. Data indicate that RMA 3CF4 clone secreted higher level of C5a than RMA 1474 clone. (B) Wildtype C57Bl/6 mice were injected with low C5a-expressing lymphoma RMA-1474 cells (n=10) or RMA CVA1 cells (n=15) and tumor growth was recorded. Data are shown as mean±s.e.m. \*p<0.05. (C) Cells from spleen and tumor from tumor-bearing mice were stained with Gr-1 and CD11b. Representative dot plots and summarized data are shown. (D) Cells were stimulated with PMA/ionomycin and surface stained with CD8 and IFN- $\gamma$  intracellularly. Representative dot plots (cells were gated on the CD8<sup>+</sup> T cells), summarized IFN- $\gamma$ -producing CD8<sup>+</sup> T cells, and total CD8<sup>+</sup> T cells are shown. (E) Cells were stimulated with PMA/ionomycin and surface stained with CD4 and IFN- $\gamma$  intracellularly. Representative dot plots (cells were gated on the CD4<sup>+</sup> T cells), summarized IFN- $\gamma$ -producing CD4<sup>+</sup> T cells, and total CD4<sup>+</sup> T cells are shown.

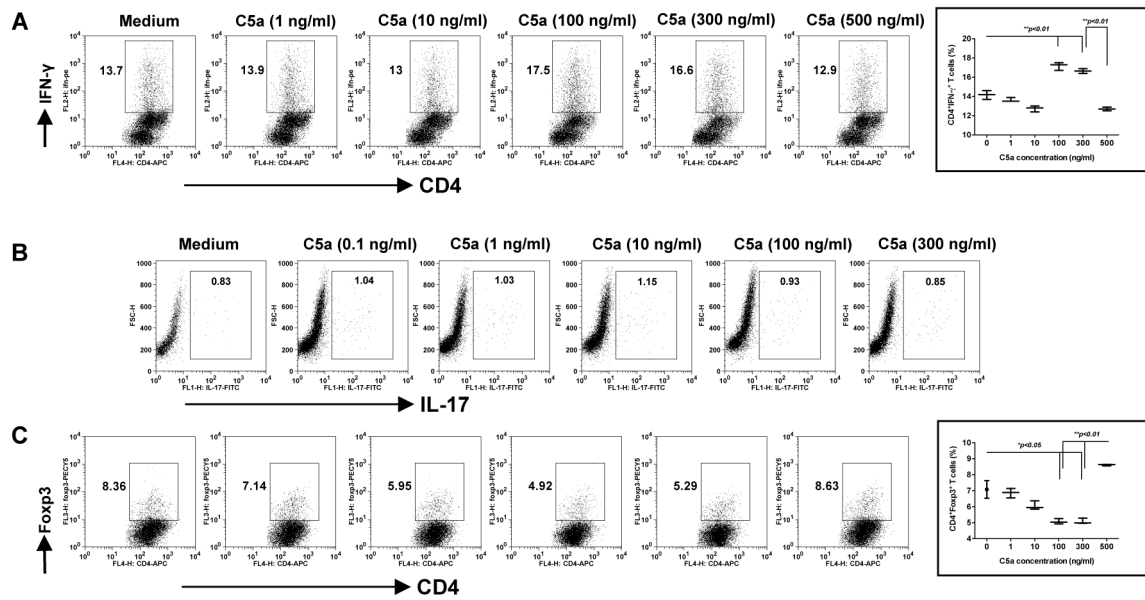


### Figure 7. C5a regulates CD4 T cell differentiation

Peritoneal macrophages were stimulated with varying concentrations of C5a (0–500 ng/ml) for 24 h and then co-cultured with naïve CD4 OVA Tg T cells in the presence of OVA for 3 days. Cells were then stained intracellularly with IFN- $\gamma$  (A) and IL-17A (B). For Treg induction assay, macrophages were co-cultured with naïve CD4 OVA Tg T cells in the presence of OVA with varying concentrations of C5a (0–500 ng/ml) for 4 days. Cells were stained intracellularly with Foxp3 (C). Representative dot plots and summarized data are shown. Cells were gated on the CD4<sup>+</sup> T cells. Data are representative of at least three independent experiments.